Contract No:

This document was prepared in conjunction with work accomplished under Contract No. 89303321CEM000080 with the U.S. Department of Energy (DOE) Office of Environmental Management (EM).

Disclaimer:

CHARGE TRAPPING EFFECTS IN THM AND VGF GROWN CdZnTeSe RADIATION DETECTORS

SRNL-STI-2022-00586

K. C. Mandal[1], S. K. Chaudhuri[1], R. Nag[1], J. W. Kleppinger[1], O. Karadavut[1], U. N. Roy[2], R. B. James[2]

[1]Dept. of Electrical Engineering, University of South Carolina, Columbia, SC 29208, USA

[2]Savannah River National Laboratory, Materials Directorate and Devices Division, Aiken, SC 29803, USA

UNIVERSITY OF South Carolina
College of Engineering and Computing

Savannah River National Laboratory®
OPERATED BY SAVANNAH RIVER NUCLEAR SOLUTIONS

MILANO
2022 IEEE NSS MIC RTSD
IEEE NUCLEAR SCIENCE SYMPOSIUM, MEDICAL IMAGING CONFERENCE AND ROOM TEMPERATURE SEMICONDUCTOR DETECTOR CONFERENCE

INTRODUCTION

- $Cd_xZn_{1-x}Te_{1-y}Se_y$ (CZTS) is a recently discovered wide bandgap (1.6 eV) high atomic number (high-Z) quaternary semiconductor.
- High bulk resistivity $\approx 3\times10^{10}$ Ω-cm.
- Excellent compositional homogeneity (both axially and radially).
- Excellent electron transport properties.
- Ideal for high energy gamma-ray detection at room temperature.

UofSC Engineering and Computing

INTRODUCTION

$Cd_xZn_{1-x}Te$ (CZT)

- Compositional inhomogeneity
- Sub-grain boundary networks
- Tellurium inclusion
- Electrically active defects

➢ Low growth yield
➢ High production cost
➢ Limits device performance

$Cd_xZn_{1-x}Te_{1-y}Se_y$ (CZTS)

- Se is added in small amount (2-3 at.%) in the CZT matrix
- Very high radial and axial compositional homogeneity
- Lower concentration of Te inclusions and other traps
- Increased mechanical hardness

➢ Crystal growth yield >90%
➢ Superior charge transport

UofSC Engineering and Computing

CZTS RADIATION DETECTORS

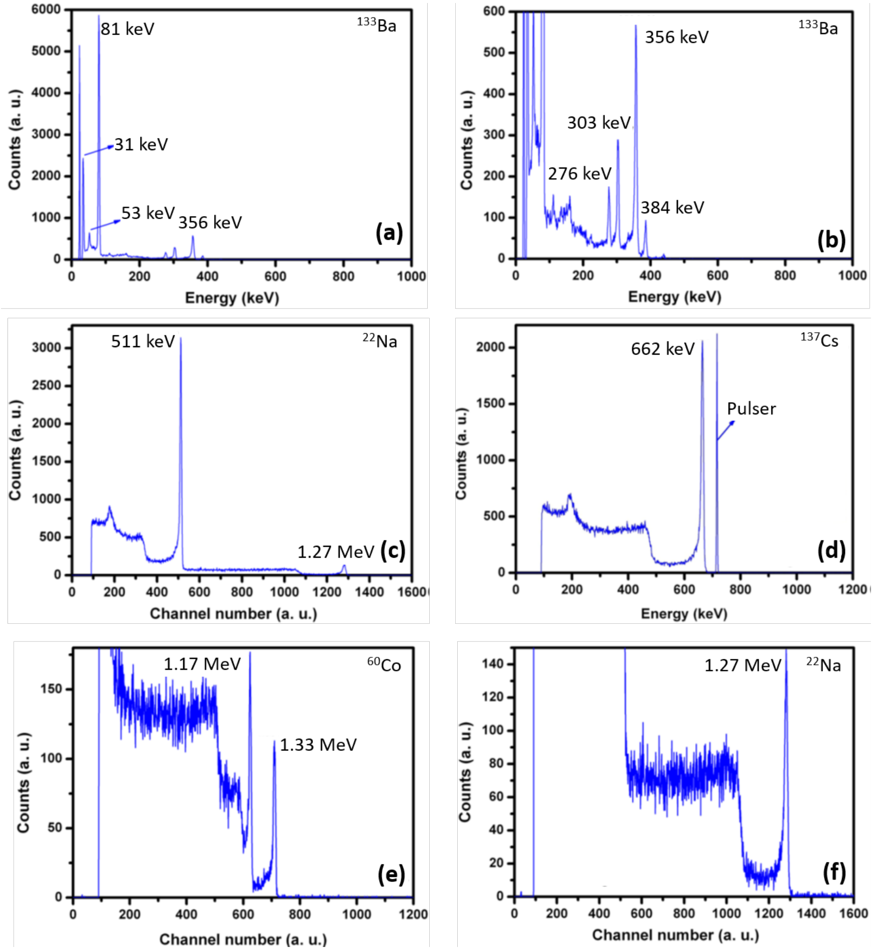

Fig: Gamma-ray pulse height spectra obtained from a THM-grown $Cd_{0.9}Zn_{0.1}Te_{0.97}Se_{0.03}$ Frisch collar detector with dimensions ~ 4.5 × 4.5 × 10.8 mm^3 with a 3-mm long Frisch grid.

Table: Reported values of energy resolution obtained using THM and VBM grown CZTS detectors in different geometries

Radioisotope	Crystal/detector type	Gamma ray energy (keV)	Energy resolution (%)
^{133}Ba	THM/Frisch collar	31	6.4 [a], 9.0 [b], 15.0 [c]
"	"	81	4.8 [a], 4.6 [b]
"	"	276	1.77 [a], 2.0 [b], 1.43 [c]
"	"	303	1.7 [a], 1.7 [b], 1.36 [c]
"	"	356	1.7 [a], 1.6 [b], 1.28 [c]
"	"	384	1.2 [a], 1.49 [c]
^{22}Na	THM/Frisch collar	511	1.34 [a], 1.26 [c]
^{137}Cs	"	662	0.9 [a], 1.07 [b], 0.77 [c]
^{137}Cs	VBM/Planar	"	2.0 [d,*]
^{22}Na	THM/Frisch collar	1275	1.0 [b], 0.56 [c]

[a] U. N. Roy, R. B. James *et al.* Appl. Phys. Lett. **114**, 232107, 2019.

[b] U. N. Roy, R. B. James *et al.* Sci. Rep. **9**, 7303, 2019.

[c] U. N. Roy, R. B. James *et al.* Sci. Rep. **11**, 10338, 2021.

[d] S. K. Chaudhuri, … K. C. Mandal, *J. Appl. Phys.* **127**, 245706, 2020.

CZTS GROWTH

Compositional Homogeneity

- Travelling Heater Method (THM)[a]
- Vertical Bridgman Method (VBM)[b]
- Horizontal Bridgman Method (HBM)[c]
- Vertical Gradient Freeze (VGF)[d,e]

[a]U. N. Roy, R. B. James *et al.,* Sci. Rep. **9**, 1620, 2019.
[b]U. N. Roy, R. B. James *et al.,* Sci. Rep. **9**, 7303, 2019.
[c]A. Yakimov *et al.,* Proc. SPIE **1114**, 111141N, 2019.
[d]L. Martínez-Herraiz *et al.,* J. Cryst. Growth **573**, 126291, 2021.
[e]R. Nag,… K. C. Mandal, J. Cryst. Growth **596**, 126826, 2022.

Vertical Gradient Freeze (VGF)

- Higher growth rate than BM and THM
- No relative motion between heater and ampoule
- No thermal drift/temperature fluctuation
- Controlled growth interface

UofSC Engineering and Computing

DETECTOR GRADE VGF GROWN CZTS

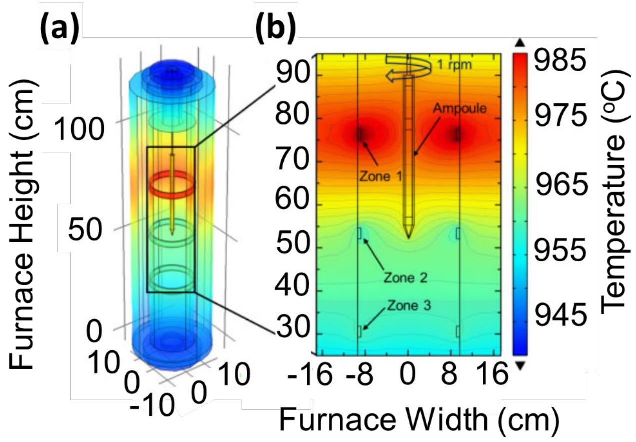

Fig. **(a)** 3D temperature distribution of the VGF furnace (simulated), and **(b)** Cross-sectional view of the temperature distribution showing the thermal gradient across the two zones.

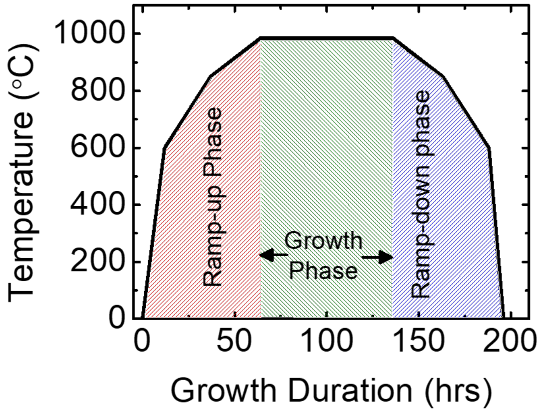

Fig. Growth profile of the crystal for the VGF growth method.

[a]R. Nag,… K. C. Mandal, J. Cryst. Growth **596**, 126826, 2022.

- $Cd_{0.9}Zn_{0.1}Te_{0.97}Se_{0.03}$ were grown at UofSC.[a]
- 5N purity Cd, Zn, Te, and Se were in-house zone-refined to obtain 7N purity elemental precursors.
- Precursors were loaded and vacuum sealed inside a 2-cm diameter carbon coated quartz tube.
- 5% excess Te and 15 ppm In (7N) were used.
- Two zones of a Lindberg Blue multizone vertical furnace were used for the crystal growth.
- Zones 1 and 2 were 20 inches apart and were set at 985 ℃ and 960 ℃, respectively.
- The total growth procedure was completed in 200 hrs.

UofSC Engineering and Computing

DETECTOR GRADE THM GROWN CZTS

- THM crystals were grown at Brookhaven National Laboratory (BNL) by Roy et al.[a]
- $Cd_{0.9}Zn_{0.1}Te_{0.98}Se_{0.02}$ was synthesized from 6N purity $Cd_{0.9}Zn_{0.1}Te$ and 6N purity CdSe precursor (pre-synthesized) materials.
- The precursors were sealed in a conically tipped quartz ampoule under vacuum (10^{-7} Torr) and loaded in a three-zone vertical furnace.
- Different lowering rates from 3 to 5 mm/day were used for the different growth runs, and the temperature gradient near the growth interface was between 10 and 15 ^{o}C/cm.
- After completion of each growth run, the ingot was cooled at a rate of 100 degrees/day.

[a]U. N. Roy, R. B. James *et al.,* Sci. Rep. **9**, 7303, 2019.

UofSC Engineering and Computing

CZTS CRYSTALS

Fig. Photograph of a CZTS ingot grown using VGF method at UofSC.

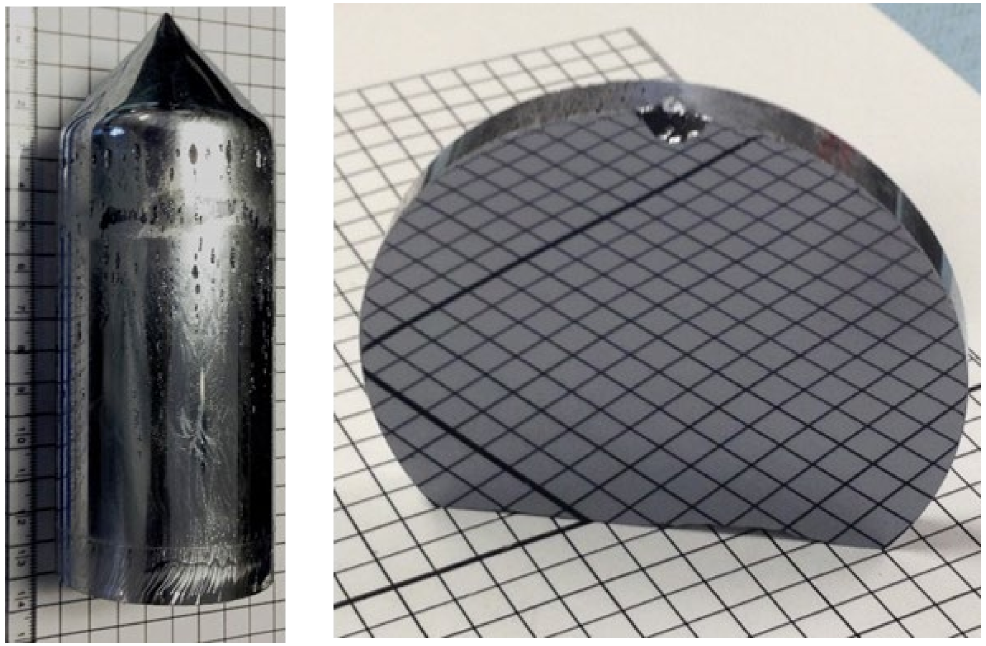

Fig. Photograph of a 2”-diameter CZTS boule and a polished wafer grown using THM at BNL.

R. Nag,… K. C. Mandal, J. Cryst. Growth **596**, 126826, 2022.

U. N. Roy, R.B. James *et al.,* Sci. Rep. **9**, 7303, 2019.

STRUCTURAL AND COMPOSITIONAL CHARACTERIZATION

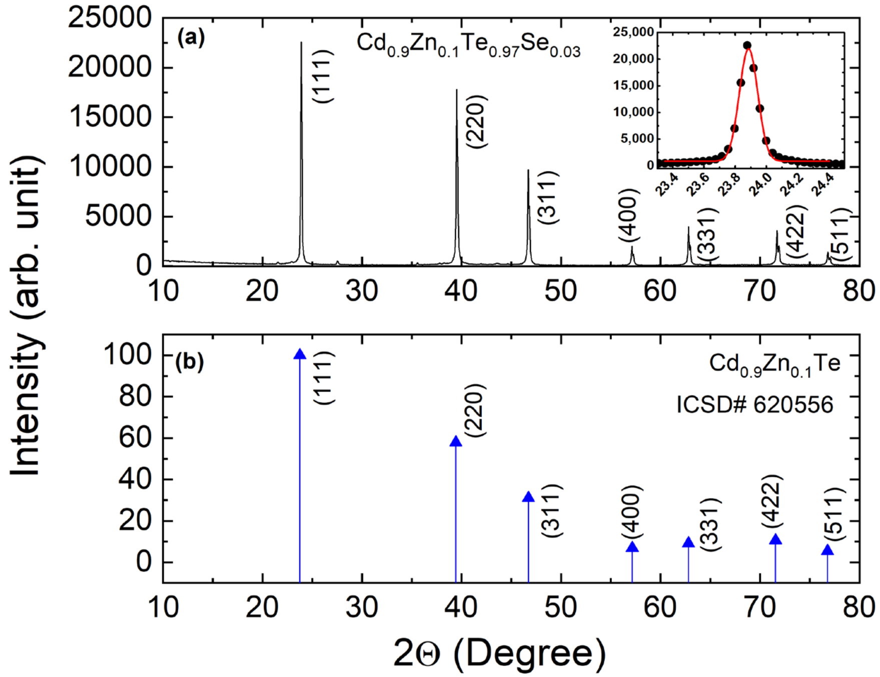

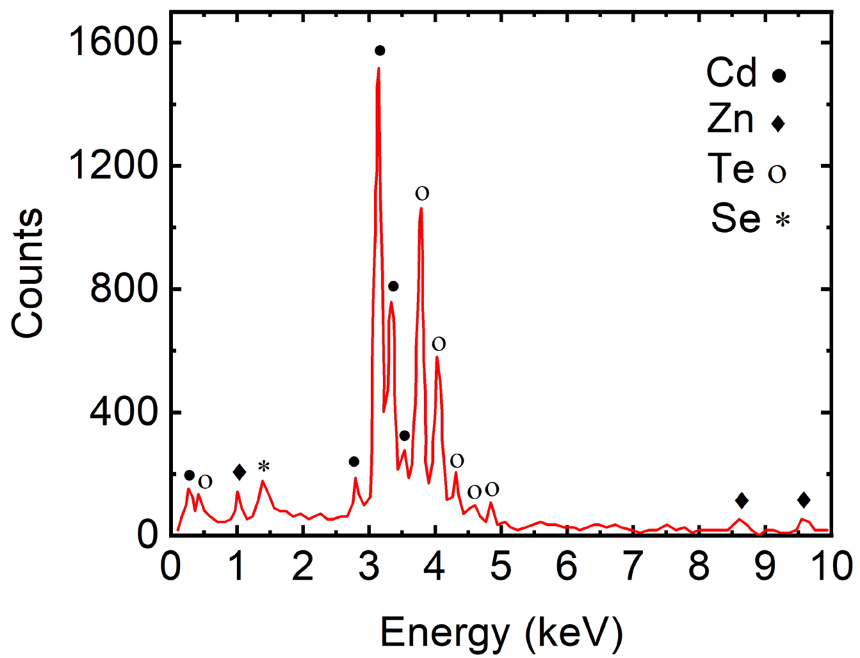

The sharp X-ray diffraction peaks with small FWHM suggest the high-quality single crystal nature of the grown material. The lattice constant a corresponding to the (111) plane was calculated to be 6.447Å.

EDX scans of the CZTS single crystals did not show the presence of any impurities. The Se/Te ratio was calculated to be 0.03 commensurate with the intended stoichiometry.

Engineering and Computing

XPS CHARACTERIZATION

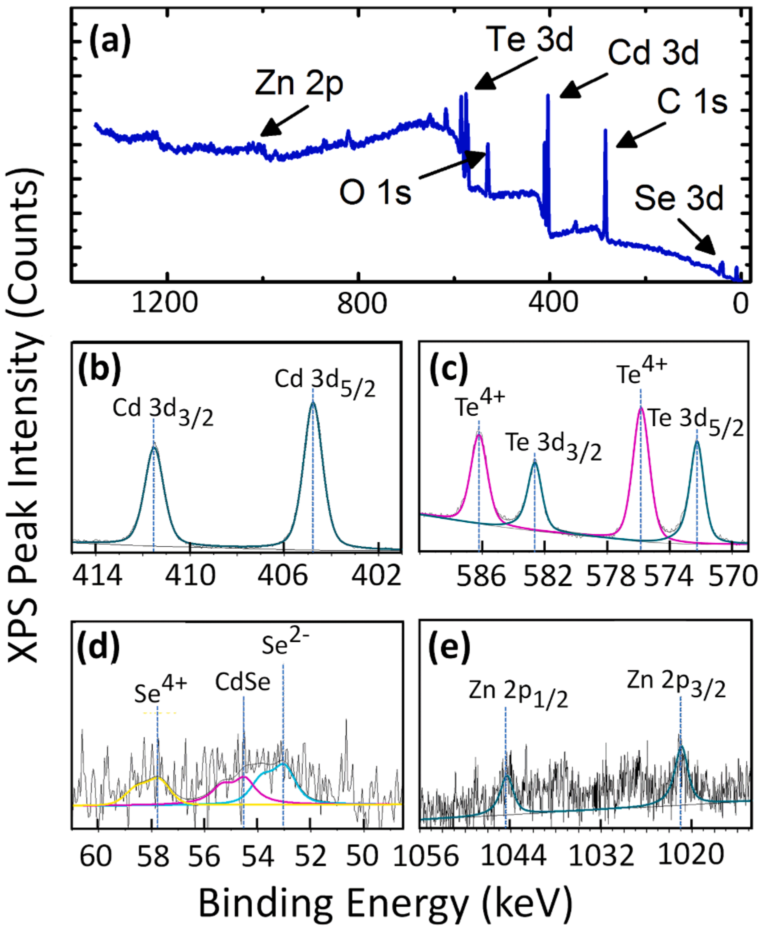

Fig. (a) XPS survey scan of the CZTS sample. High resolution core level spectra of Cd 3d **(b)**, Te 3d **(c)**, Se 3d **(d)**, and Zn 2p **(e)** states.

- Spectral lines of Cd, Te, Zn, and Se were observed.
- No impurity related peaks were observed in the survey scan.
- The Cd^{2+}, Te^{2-}, Se^{2-}, and Zn^{2+} oxidation states were observed.
- O-Te and Se-O bonding were also observed.
- The XPS measurements confirmed the formation of the desired bonds and hence the formation of the CZTS quaternary compound.

UofSC Engineering and Computing

TELLURIUM INCLUSIONS

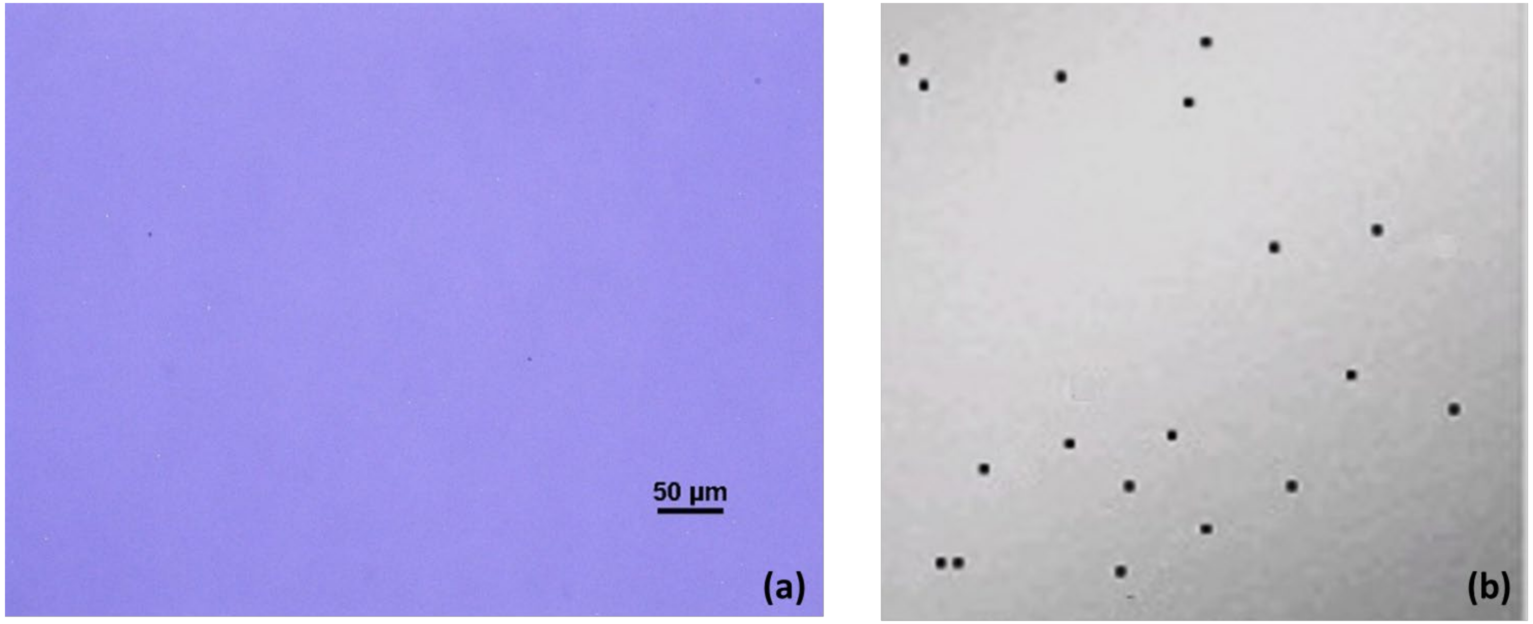

Fig. Infrared transmission images showing the Te inclusions obtained for **(a)** THM- and **(b)** VGF-grown CZTS single crystals.

- The concentrations of Te inclusions were calculated to be 4.3×10^4 and 8×10^5 cm^{-3} for the THM and the VGF crystals, respectively.
- Although the density of the Te inclusions appears to be larger in comparison to the THM-grown crystals, the size of the Te inclusions in the VGF-grown crystal were less than 10 µm.

UofSC Engineering and Computing

ELECTRICAL CHARACTERIZATION

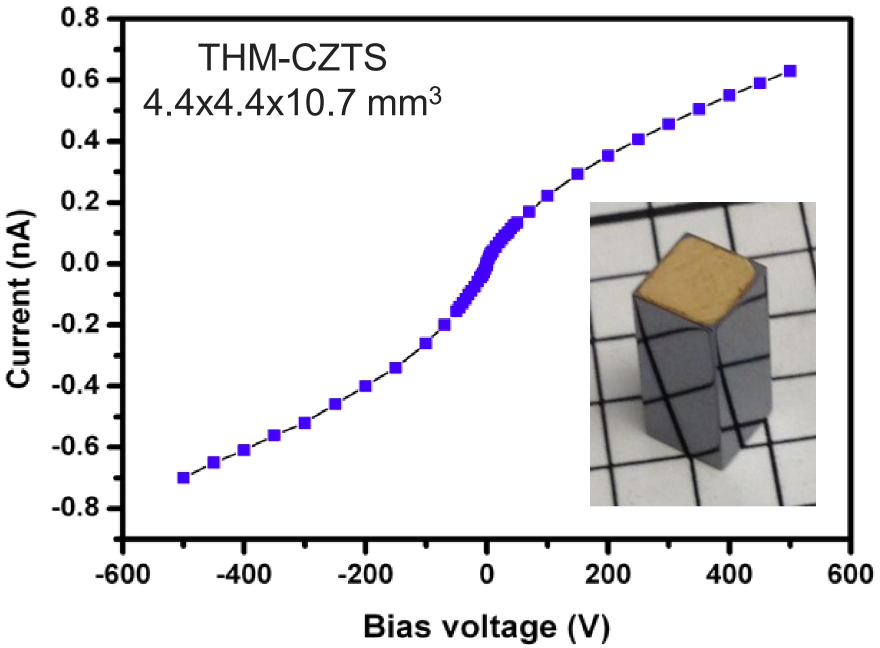

Fig. Current-voltage (*I-V*) characteristics recorded under dark and at room temperature in a planar configuration.

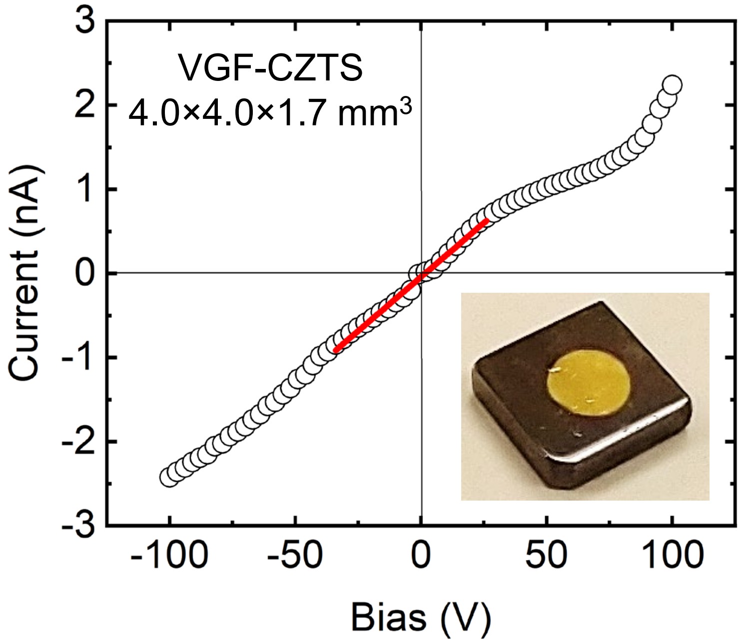

- The bulk electrical resistivity was calculated to be 2.9×10^{10} Ω.cm and 1.6×10^{10} Ω.cm for the THM- and the VGF-grown crystals.
- A slight asymmetry of the *I-V* characteristics with respect to the bias polarity at higher voltages was observed, which is due to the difference in properties of the two surfaces.

Engineering and Computing

CHARGE TRANSPORT MEASUREMENTS

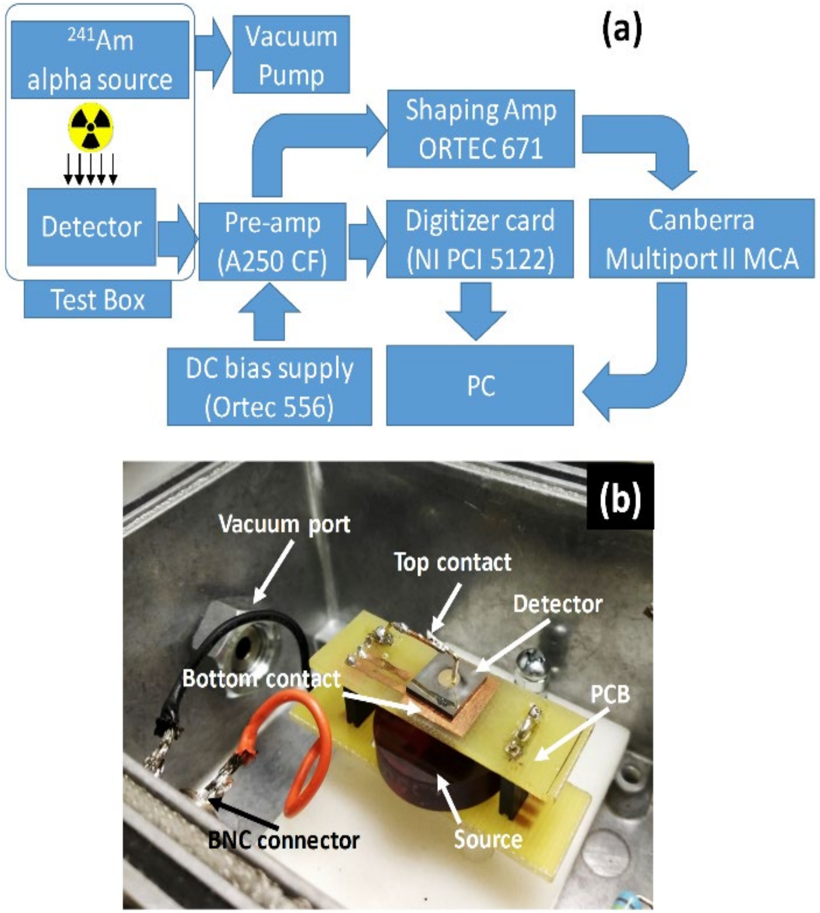

Fig. (a) Alpha spectrometer (analog/digital) configuration for the charge transport property measurements. **(b)** A typical detector-source arrangement for the alpha spectroscopic measurements.

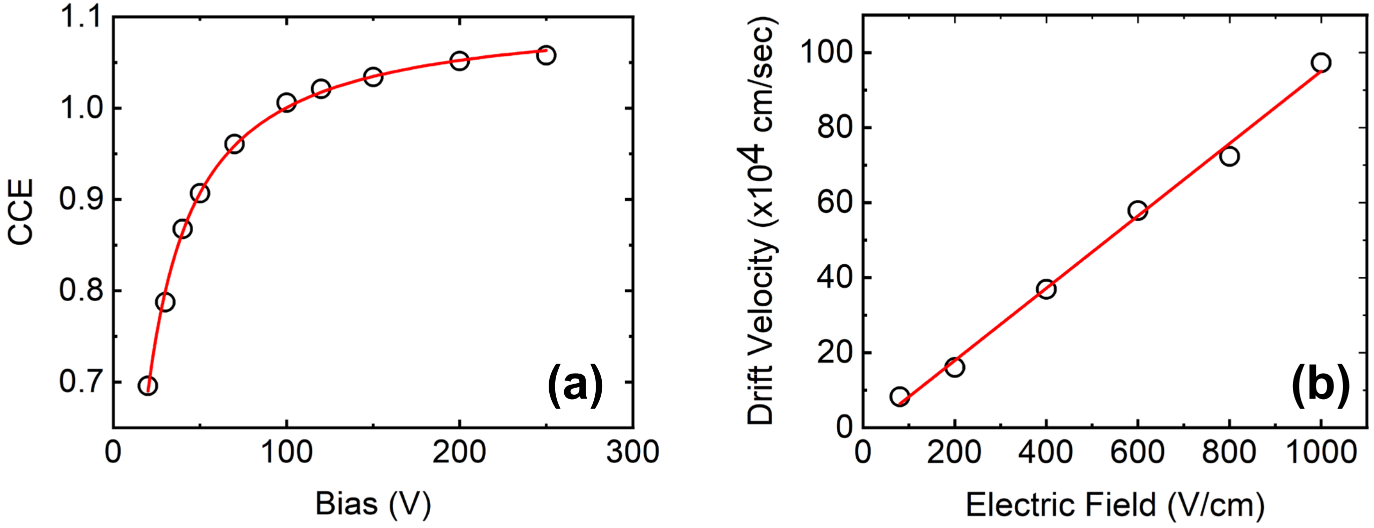

Fig. Hecht **(a)** and drift-mobility **(b)** plots obtained for a VGF-grown CZTS planar detector.

- The $\mu\tau$ product for the electrons calculated from the Hecht plot was found to be 3 × 10^{-3} cm^2/V and 6 × 10^{-3} cm^2/V for the VGF and the THM grown CZTS sample, respectively.
- The electron drift mobility was calculated to be 964 $cm^2/V.s$ and 830 $cm^2/V.s$ for the VGF and the THM grown CZTS sample, respectively.

Engineering and Computing

GAMMA RAY DETECTION

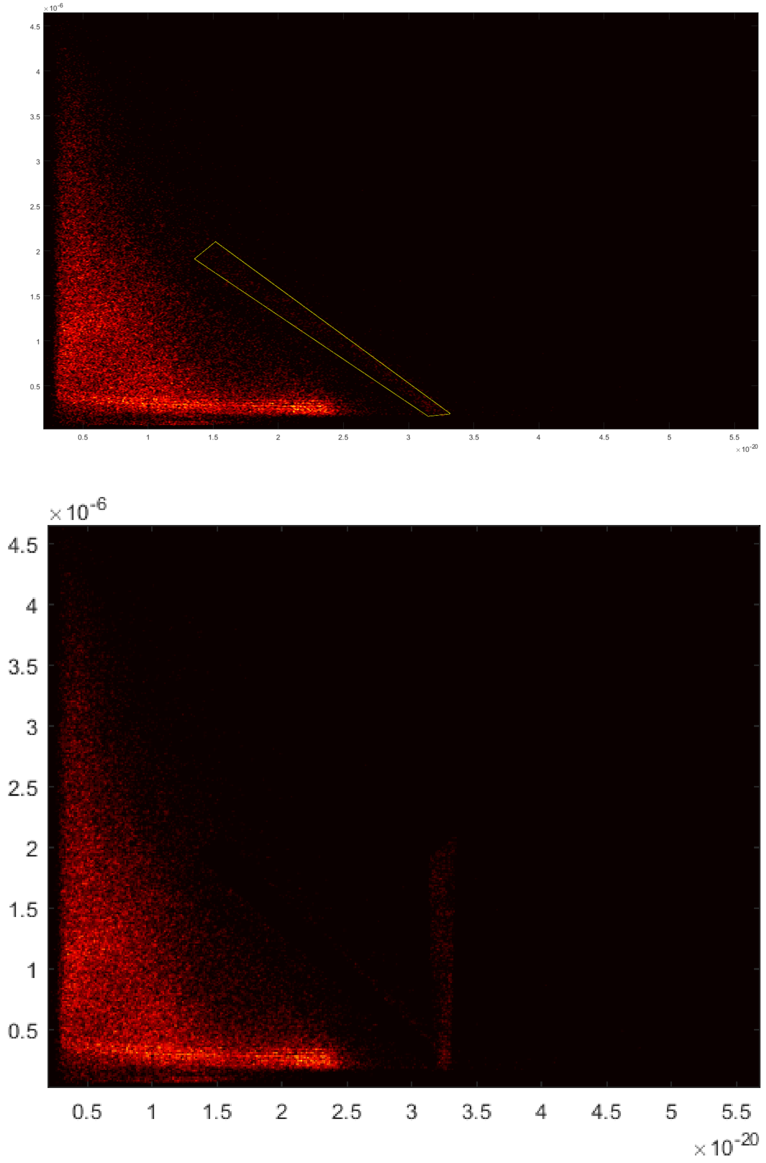

Fig. Biparametric (BP) plots obtained before (top) and after (bottom) digital correction.

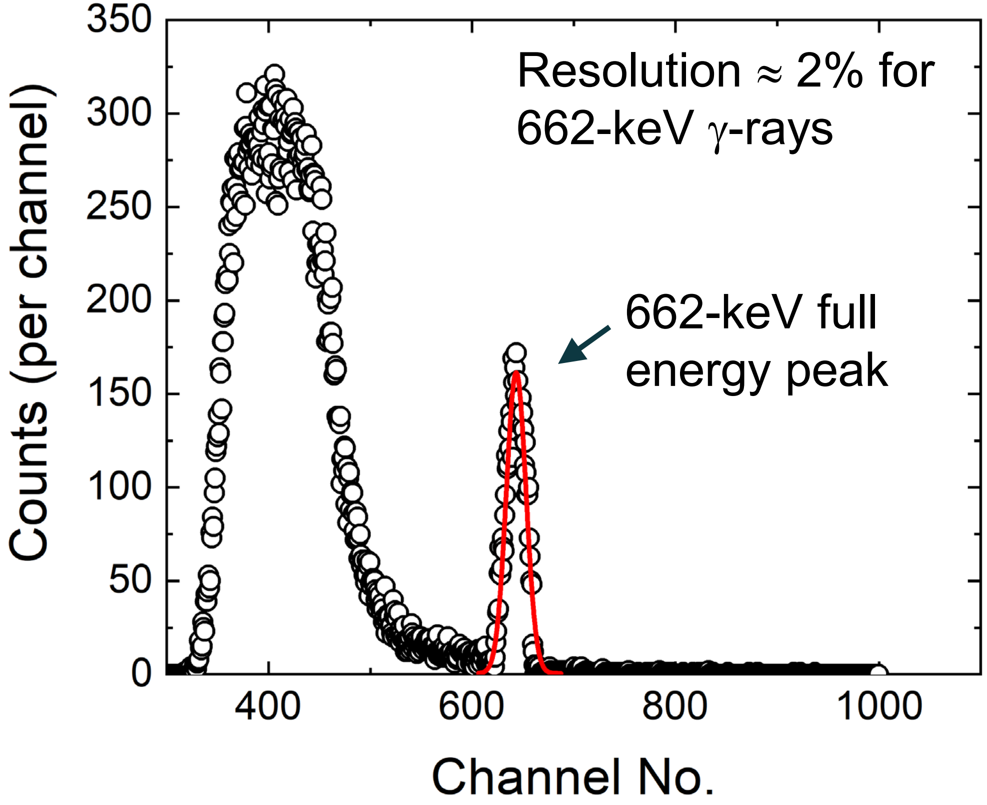

Fig. Pulse height spectrum obtained by exposing a VGF-grown CZTS crystal to a ^{137}Cs source after digital BP correction.

UofSC Engineering and Computing

DEFECT CHARACTERIZATION

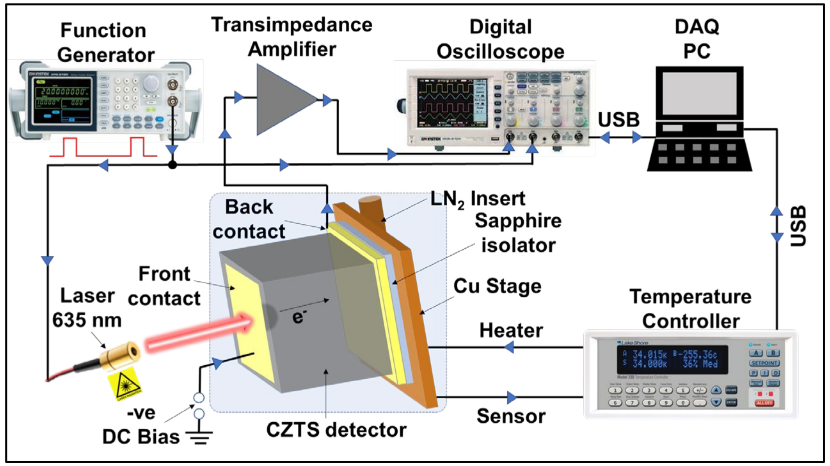

Fig. Schematic of the photo-induced current transient spectroscopy (PICTS) set-up at UofSC.

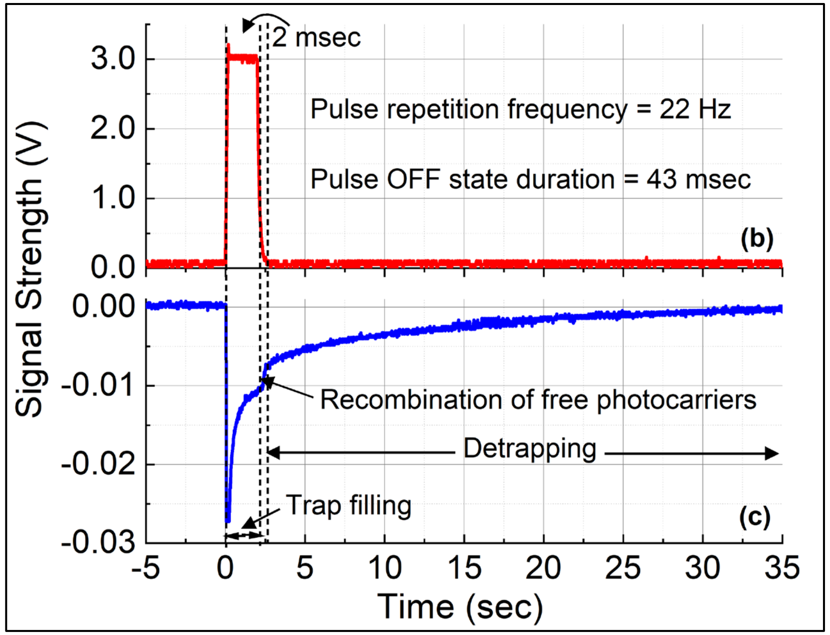

Fig. An excitation pulse used for saturation trap filling (top). A typical PICTS signal obtained at room temperature for the VGF-grown CZTS detector (bottom).

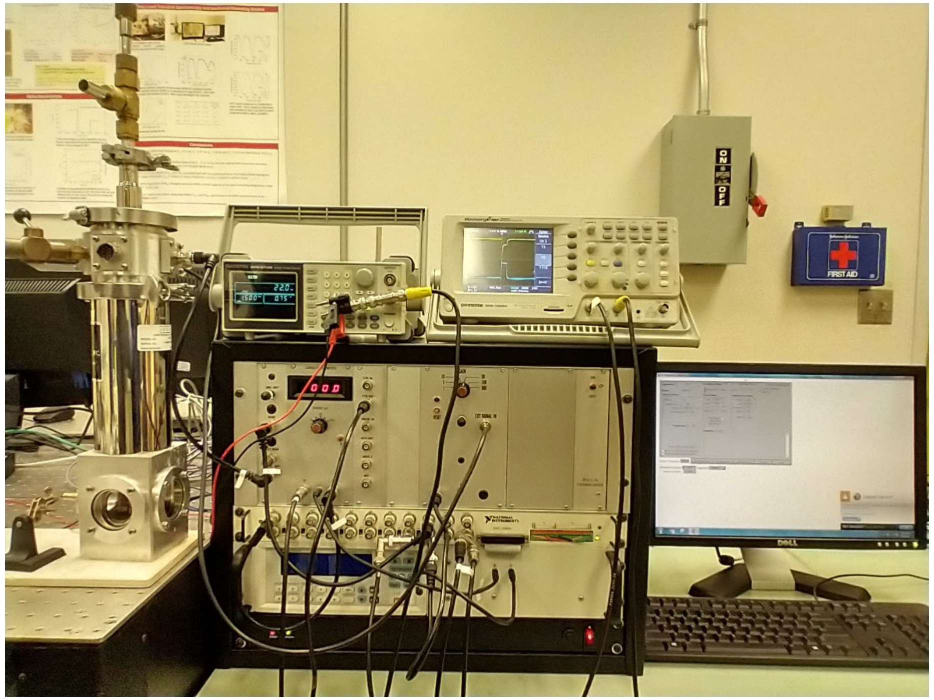

Fig. A photograph of the Sula Technologies DLTS set up at UofSC configured for PICTS measurements.

Engineering and Computing

PICTS RESULTS

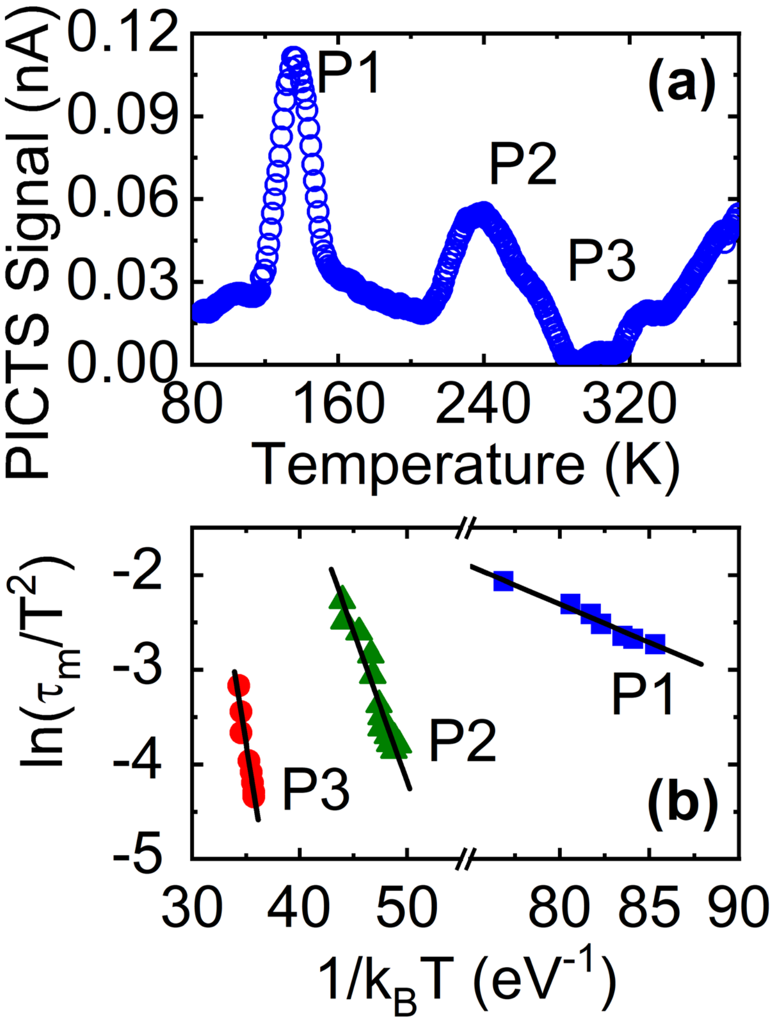

Fig. (a) A PICTS spectrum recorded for a VGF-grown $Cd_{0.9}Zn_{0.1}Te_{0.98}Se_{0.03}$ detector in the temperature scan range 85 – 400 K. **(b)** The Arrhenius plot corresponding to the peaks PI, P2, and P3 observed in the PICTS scans.

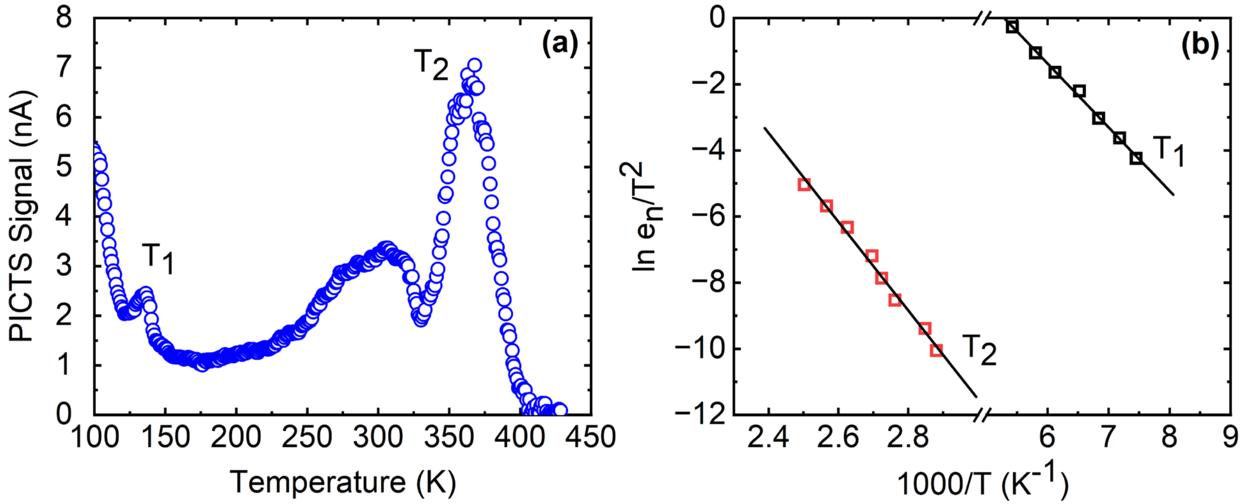

Fig. (a) A PICTS spectrum recorded for a THM-grown $Cd_{0.9}Zn_{0.1}Te_{0.98}Se_{0.02}$ detector in the temperature scan range 85 – 400 K. **(b)** The Arrhenius plot corresponding to the peaks PI, P2, and P3 observed in the PICTS scans.

Defect parameters	P1	P2	P3	T1	T2
E_C - E_T (eV)	0.08	0.32	0.72	0.16	1.14
Concentration (cm^{-3})	$\sim 10^{11}$	$\sim 10^{11}$	$\sim 10^{11}$	9.78×10^{10}	6.59×10^{11}

Engineering and Computing

CONCLUSION

- CZTS single crystals have been grown using a THM (2-3% at.) and a VGF (3% at.) method.
- All the crystals showed resistivity on the order of 10^{10} Ω.cm.
- The charge transport properties were similar in both types of CZTS crystal.
- The concentration of Te inclusions was higher in the VGF-grown CZTS.
- PICTS results showed different types of trap centers in the two differently grown CZTS crystals.
- High energy (662 keV) gamma rays with decent energy resolution were detected using a planar detector fabricated from the VGF-grown CZTS crystals.

UofSC Engineering and Computing

FUTURE STUDIES

- Identification of the defects observed in the PICTS spectra using DFT calculations
- Comparison of THM- and VGF-grown CZTS crystals with same atomic percentage of Selenium
- Fabrication of small-pixel detector using VGF-grown CZTS crystals for single-polarity gamma detection
- Correlation of charge trapping centers with device performance

UofSC Engineering and Computing

ACKNOWLEDGEMENT

- The authors acknowledge the partial financial support from the Laboratory Directed Research and Development (LDRD) program within the Savannah River National Laboratory (SRNL) under Contract No. 89303321CEM000080.
- The authors acknowledge the assistance of the Electron Microscopy Center at UofSC for the SEM and EDX measurements.
- The authors thank Dr. Stavros G. Karakalos, Dept. of Chemical Engineering, College of Engineering and Computing at UofSC for the XPS measurements and analysis.

UofSC Engineering and Computing

THANK YOU!